Selection in Heavy Ion Collisions Through Event Shape Engineering

Zhiyan Yu

School of Art and Sciences, University of Rochester, Rochester, 14627, USA

zyu25@u.rochester.edu

Abstract. This study uses Glauber Monte Carlo simulations to investigate the connection between initial collision geometry and potential jet quenching effects. A dataset of 75,000 simulated collision events was examined, with a focus on the associations between geometrical parameters such as participant numbers, eccentricity, triangularity, and their respective orientation angles, and the impact parameters. By calculating path length differences for each event, optimal ranges of such variables were identified, which could possibly enhance observable jet quenching. Our findings show that mid-central collisions with 100 to 200 participants, higher eccentricity, and impact parameters of 8 fm provide the optimal conditions for studying path length-dependent phenomena.

Keywords: Glauber Monte Carlo simulations, Heavy ion collisions, Event shape engineering

1 Introduction

The Glauber Monte Carlo model is a computational technique to simulate the initial geometry of heavy ion collisions. The colliding nuclei are modeled through random distribution of nucleons with probabilities determined by measured nuclear density profiles [1]. These are then ”collided” by overlapping them at a uniformly distributed random impact parameter whereby nucleon-nucleon collisions were determined based on the geometrical cross-section [2].

This simulation calculates several important quantities, including the number of participating nucleons N_{part} [3], the impact parameter b, the eccentricity and triangularity of the overlap region ϵ_2 and ϵ_3 [4], and the angle between the shortest axis of the elliptical shape and orientation of the triangular shape in the initial collision geometry ψ_2 and ψ_3. By running multiple simulated collisions, the model generates distributions of these quantities that can be compared to experimental results.

The Glauber Monte Carlo model is important for interpreting data from heavy ion collisions and understanding how initial geometry influences the evolution of the quark-gluon plasma formed in such events. This model links experimentally observed particle multiplicities to the initial collision geometry, making it a vital tool for heavy ion collision data analysis.

Event-by-event fluctuations in these collisions are essential for understanding the complex dynamics of such systems [5]. These fluctuations involve variations in initial geometry, energy density, and other properties from one collision to another. They originate from the quantum mechanical nature of colliding nuclei and the probabilistic nature of nucleon-nucleon interactions [6].

CONF-CIAP 2025, January 17-23, Eskisehir, Turkey

DOI 10.4108/eai.17-1-2025.2355243

The significance of these fluctuations is multifaceted. They heavily influence the initial state geometry, leading to differences in the shape and size of the interaction region [7]. This affects the initial spatial eccentricity, which is a key factor driving collective flow in the quark-gluon plasma as it expands [8]. Flow patterns observed, especially higher-order harmonics, are particularly sensitive to these initial state fluctuations. As discussed in Ref [9], the ratio of triangular flow to elliptic flow increases for more central collisions and higher transverse momentum particles, a trend that aligns with observations in experimental data. By studying these flow patterns, we can gain insights into the initial state geometry and the subsequent hydrodynamic evolution of the system.

Knowing the importance of event-by-event fluctuations, one can study the correlations among variables through event shape engineering [10]. This technique allows us to exploit the natural event-by-event fluctuations in heavy ion collisions by selecting events with specific initial geometry configurations. It provides a unique opportunity to isolate and study the effects of initial state geometry on the evolution and properties of the quark-gluon plasma.

2 Data and Analysis

To study event-by-event fluctuations, a large enough data set is required for representative behaviors. Therefore, a data set consisting of 75000 independent events generated through Glauber MC is applied in the experiment. To keep the data points in a reasonable region, impact parameter b is set to be within 0-12 and the number of participants is set to be above 50.

It would be reasonable to ask how the main variables relate. If some innate correlations were found, reducing them into expressions of other variables to simplify the model is beneficial. This can be primarily done through 2D histograms.

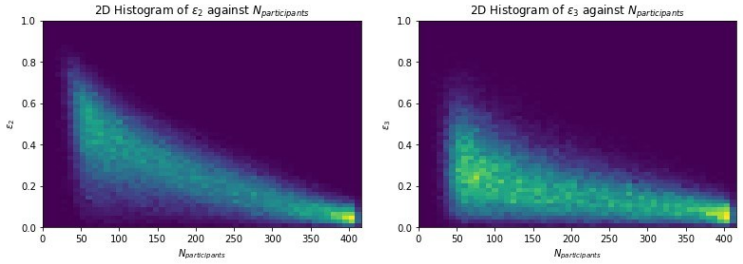

(a) Correlation between ϵ_2 and *Npart* (b) Correlation between ϵ_3 and *Npart*

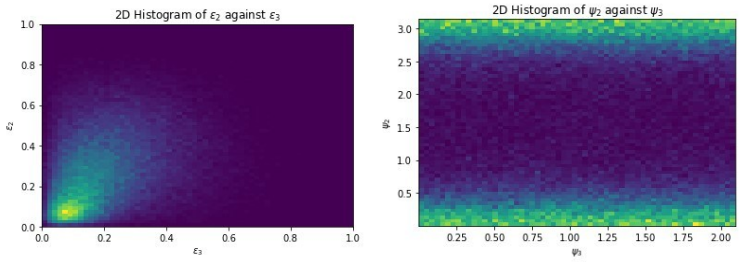

(c) Correlation between ϵ_2 and ϵ_3 (d) Correlation between ψ_2 and ψ_3

Fig. 1. 2D histograms of dependence among variables

Shown in Figure 1, the correlations among important variables are intuitive to observe. There's a weak dependence both between ϵ_2 and N_{part} and between ϵ_3 and N_{part}. This is mainly due to the nature of these variables, where lower values of ϵ_2 and ϵ_3 usually show that head-on collisions are more likely to happen. This situation will naturally result in a larger N_{part}, which aligns with the findings in (a) and (b). In (c), the correlation between ϵ_2 and ϵ_3 is relatively weak since they are highly concentrated in lower values and diffuse in all directions. In (d), distribution is primarily uniform, and no correlations between ψ_2 and ψ_3 were found. This method can be applied to any other variable combination, though these correlations are the most likely to occur.

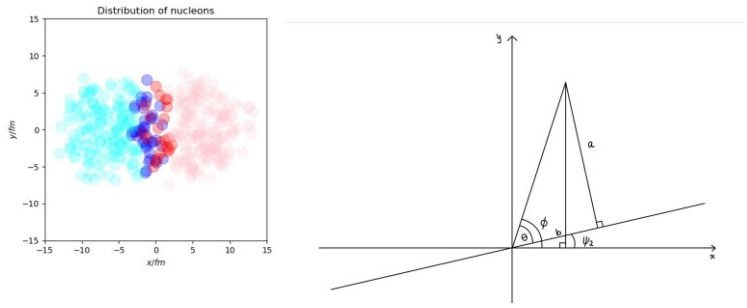

(a) Diagram of a single event. (b) Geometry of a single nucleon.

Fig. 2. (a) a random collision event that shows the distribution inside the participating nuclei. The blue and red units are the participating nucleons from nuclei 1 and 2, whereas cyan and pink units are the spectators from nuclei 1 and 2 respectively. (b) shows the position of each nucleon relative to the center of the collision.

To actively select conditions that maximize the jet quenching effect, the path lengths and path length differences for each collision event must be calculated. This is achieved by counting the number of participants in contact with the major and minor axes of the ellipse formed by the participants. This can be done by drawing the two axes and counting the number of nucleons they travel through, or by geometry and trigonometry.

As shown in Figure 2, geometry is applied in this case. Since we can calculate the position of the center of collision, the relative position of each nucleon to the center can be calculated using diagram (b). $\phi = \arctan\left(\frac{y_{diff}}{x_{diff}}\right)$, so $\theta = \phi - \psi_2$.

Therefore, we have:

$$a = \sqrt{y_{diff}^2 + x_{diff}^2} \cdot \sin(\theta) \tag{1}$$

$$b = \sqrt{y_{diff}^2 + x_{diff}^2} \cdot \cos(\theta) \tag{2}$$

Hence, the nucleon is said to intersect with the axes if a or b is equal to or less than the radius of the nucleon. If a is less than the radius, $N_{parallel}$ increases by 1, and vice versa. Finally, $\Delta N = N_{perpenducular} - N_{parallel}$. Radius is calculated using $\sigma_{NN} = 42mb$ and $D = \sqrt{\frac{\sigma_{NN}}{\pi}}$ [1].

After applying this to every event, the relationships between ΔN and other variables can be studied. Instead of plotting 2D histograms like how it was done previously, each variable is

divided into 10 bins, and the average of ΔN is taken in each bin. Therefore, line charts of $< \Delta N >$ against each variable can be plotted.

According to Figure 3, each variable has a different impact on ΔN. General predictions can be made based on the line charts. The average peaks when

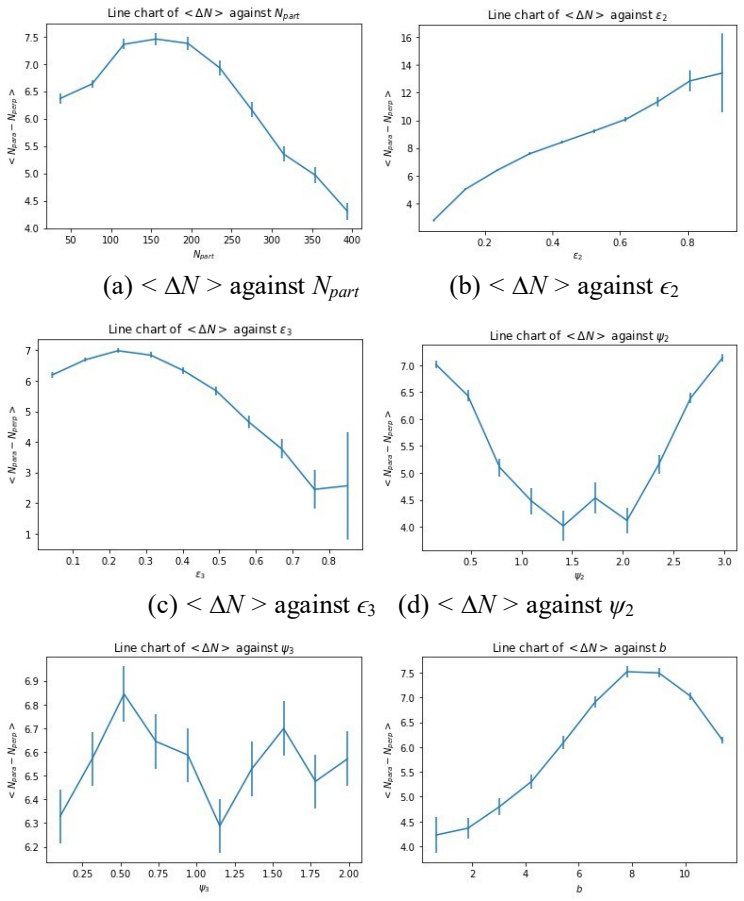

(a) $< \Delta N >$ against N_{part} (b) $< \Delta N >$ against ϵ_2

(c) $< \Delta N >$ against ϵ_3 (d) $< \Delta N >$ against ψ_2

(e) $< \Delta N >$ against ψ_3 (f) $< \Delta N >$ against b

Fig. 3. Line charts of dependence between $< \Delta N >$ and other variables. The uncertainties are calculated by: $\frac{rms}{\sqrt{n}}$, where rms is the root mean square value of each bin and n is the number of events enclosed in the corresponding bin.

N_{part} is between 100 and 200, with relatively small error bars, indicating that selections with N_{part} in this range are preferred. Higher values of ϵ_2 results in high averages. Though the error rises, an increasing trend can still be seen. The same method can be applied to four other plots. One can discover that the average peaks when ϵ_3 is around 0.2, ψ_2 is < 0.5 or > 2.7, and b is around 8. The only exception is ψ_3, where most error bars overlap with others and the differences between two points are very small. Therefore, one can conclude that the dependence of $< \Delta N >$ on ψ_3 is weak.

With the predictions, the dependence of the average on all variables can be studied. The same approach can be taken except for bin sizes. Each parameter is divided into four bins to avoid having only one or two events in each bin. Results can be sorted by $< \Delta N >$, and the 40 events with the highest average values are shown in Table 1.

Table 1. 40 events with highest $< \Delta N >$.

$< \Delta N >$	$\Delta < \Delta N >$	*Npart*	ϵ_2	ϵ_3	ψ_2	ψ_3	*b*
31.000000	31.000000	3.0	3.0	1.0	1.0	3.0	2.0
28.000000	28.000000	2.0	3.0	2.0	3.0	4.0	3.0
25.000000	25.000000	4.0	1.0	2.0	3.0	4.0	1.0
23.000000	23.000000	2.0	3.0	1.0	2.0	1.0	4.0
23.000000	23.000000	2.0	2.0	3.0	3.0	4.0	3.0
23.000000	23.000000	3.0	1.0	3.0	3.0	2.0	3.0
22.000000	22.000000	1.0	3.0	1.0	4.0	1.0	3.0
21.000000	21.000000	3.0	2.0	1.0	3.0	4.0	3.0
21.000000	21.000000	4.0	2.0	1.0	1.0	3.0	1.0
21.000000	21.000000	3.0	2.0	1.0	3.0	3.0	3.0
20.000000	20.000000	2.0	3.0	3.0	4.0	2.0	3.0
20.000000	20.000000	1.0	3.0	2.0	4.0	1.0	3.0
19.000000	19.000000	1.0	4.0	1.0	3.0	3.0	4.0
18.500000	13.086252	1.0	4.0	2.0	3.0	1.0	4.0
18.500000	13.124405	1.0	3.0	1.0	4.0	3.0	3.0
18.000000	18.000000	4.0	2.0	2.0	3.0	4.0	2.0
18.000000	18.000000	1.0	2.0	1.0	4.0	3.0	3.0
18.000000	18.000000	4.0	1.0	2.0	4.0	3.0	1.0
18.000000	18.000000	1.0	3.0	2.0	1.0	1.0	3.0
17.500000	3.780891	2.0	3.0	2.0	1.0	1.0	3.0
17.000000	17.000000	3.0	2.0	1.0	2.0	1.0	3.0
17.000000	12.041595	1.0	3.0	2.0	4.0	4.0	3.0
17.000000	17.000000	1.0	4.0	2.0	2.0	2.0	4.0
16.661538	2.208697	2.0	3.0	1.0	4.0	4.0	3.0
16.500000	11.672618	1.0	3.0	1.0	1.0	3.0	3.0
16.173913	3.719361	2.0	3.0	2.0	4.0	2.0	3.0
16.000000	16.000000	3.0	2.0	1.0	3.0	4.0	2.0
15.789474	3.929433	2.0	3.0	2.0	4.0	4.0	4.0
15.571429	6.345495	4.0	2.0	1.0	4.0	3.0	2.0
15.518519	2.245098	2.0	3.0	1.0	4.0	3.0	3.0
15.315789	3.767848	2.0	3.0	2.0	4.0	1.0	3.0
15.200000	8.094443	4.0	2.0	1.0	1.0	1.0	2.0

Table 1. (continued).

15.000000	15.000000	1.0	4.0	2.0	3.0	2.0	4.0
15.000000	15.000000	1.0	4.0	1.0	2.0	1.0	4.0
15.000000	6.155395	1.0	3.0	3.0	2.0	2.0	4.0
14.947368	3.676684	2.0	3.0	2.0	1.0	4.0	3.0
14.777778	2.226693	2.0	3.0	1.0	4.0	2.0	3.0
14.731707	2.411059	2.0	3.0	1.0	4.0	3.0	4.0
14.621622	2.600079	2.0	3.0	1.0	1.0	4.0	3.0
14.612245	2.220648	2.0	3.0	1.0	1.0	2.0	3.0

The uncertainties are calculated by: $\frac{rms}{\sqrt{n}}$, where rms is the root mean square value of each bin and n is the number of events enclosed in the corresponding bin.

The uncertainties of the first several bins are high since only one event was enclosed. Ruling out these statistical fluctuations, it's pretty clear that N_{part} falls in bin 2, meaning that it should be 25% to 50% of the range, which is consistent with our previous prediction of 100 to 200. Meanwhile, ϵ_2 are in bin 3, ϵ_3 are in bin 1, ψ_2 are in bin 4, ψ_3 do not have a particular pattern, and b are in bin 3, which agree with our previous predictions.

3 Interpretation

The analysis of event-by-event fluctuations in heavy ion collisions using the Glauber Monte Carlo model reveals several important insights into the initial geometry of these collisions and their impact on observable quantities.

The weak dependence observed between eccentricity ϵ_2 and participant number N_{part}, as well as between triangularity ψ_3 and N_{part}, aligns with our understanding of collision geometry. Lower eccentricity and triangularity values typically correspond to more central collisions, which naturally involve a larger number of participants. This relationship underscores the connection between the impact parameter and the shape of the interaction region.

The calculation of path length differences $< \Delta N >$ provides a crucial link between initial geometry and potential jet-quenching effects. The observed relationships between $< \Delta N >$ and various geometric parameters offer valuable insights:

1. The peak in $< \Delta N >$ for N_{part} between 100 and 200 suggests that midcentral collisions may provide the optimal conditions for studying path length effects on jet quenching.
2. The positive correlation between $< \Delta N >$ and ϵ_2 indicates that more elliptical collision geometries lead to larger path length differences, potentially enhancing observable jet quenching effects.
3. The weak dependence of $< \Delta N >$ on ψ_3 implies that the orientation of triangularity has minimal impact on path length differences, focusing our attention on ellipticity as the primary driver of these effects.

4 Conclusions

This study demonstrates the power of event shape engineering techniques in heavy ion collisions using Glauber Monte Carlo simulations. By analyzing the correlations between various geometric parameters and their impact on path length differences, we have gained valuable insights into the initial state geometry of these collisions and their potential effects on observable quantities.

Future work may incorporate these event shape engineering techniques into full hydrodynamic simulations to study the evolution of the quark-gluon plasma under specific initial geometry conditions [11]. More sophisticated event selection algorithms that can efficiently identify and categorize events based on multiple geometric criteria can be developed.

References

[1] Alver, B. H., Baker, M. D., Loizides, C., and Steinberg, P. (2008). The PHOBOS Glauber Monte Carlo.

[2] Loizides, C., Kamin, J., & d'Enterria, D. (2018). Improved monte carlo glauber predictions at present and future nuclear colliders. Physical Review C, 97(5). https://doi.org/10.1103/physrevc.97.054910

[3] Konchakovski, V. P., Gorenstein, M. I., Bratkovskaya, E. L., & Greiner, W. (2010). Fluctuations and correlations in nucleus–nucleus collisions within transport models. Journal of Physics G: Nuclear and Particle Physics, 37(7), 073101. https://doi.org/10.1088/0954-3899/37/7/073101

[4] Mazeliauskas, A., & Teaney, D. (2015). Subleading harmonic flows in hydrodynamic simulations of heavy ion collisions. Physical Review C, 91(4). https://doi.org/10.1103/physrevc.91.044902

[5] Stephanov, M., Rajagopal, K., & Shuryak, E. (1999). Event-by-event fluctuations in heavy ion collisions and the QCD critical point. Physical Review D, 60(11). https://doi.org/10.1103/physrevd.60.114028

[6] An, X., Başar, G., Stephanov, M., & Yee, H.-U. (2020). Fluctuation dynamics in a relativistic fluid with a critical point. Physical Review C, 102(3). https://doi.org/10.1103/physrevc.102.034901

[7] Bhalerao, R. S., Ollitrault, J.-Y., Pal, S., & Teaney, D. (2015). Principal component analysis of event-by-event fluctuations. Physical Review Letters, 114(15). https://doi.org/10.1103/physrevlett.114.152301

[8] Jia, J., & Huo, P. (2014). Forward-backward eccentricity and participant-plane angle fluctuations and their influences on longitudinal dynamics of collective flow. Physical Review C, 90(3). https://doi.org/10.1103/physrevc.90.034915

[9] Alver, B., and Roland, G. (2010). Collision-geometry fluctuations and triangular flow in heavy-ion collisions. Physical Review C, 81(5).https://doi.org/10.1103/physrevc.81.054905

[10] Jia, J. (2022). Shape of atomic nuclei in heavy ion collisions. Physical Review C, 105(1). https://doi.org/10.1103/physrevc.105.014905

[11] Kumar, R., Dexheimer, V., Jahan, J. et al. Theoretical and experimental constraints for the equation of state of dense and hot matter. Living Rev Relativ 27, 3 (2024). https://doi.org/10.1007/s41114-024-00049-6